Purdue University

Purdue e-Pubs

International Compressor Engineering Conference

School of Mechanical Engineering

2021

Experimental Investigation of an Optimized Mechanically Assisted Suction Reed Valve of a Hermetic Reciprocating Compressor

Andreas Egger
Graz University of Technology, Austria, egger@ivt.tugraz.at

Raimund Almbauer

Michael Lang

Christoph Zainer

Experimental Investigation of an Optimized Mechanically Assisted Suction Reed Valve Design Concept in a Small Hermetic Reciprocating Compressor

Andreas EGGER[1]*, Raimund ALMBAUER[1], Michael LANG[1], Christoph ZAINER[1]

[1]Graz University of Technology, Institute of Internal Combustion Engines and Thermodynamics,
Inffeldgasse 19, 8010 Graz, Austria
egger@ivt.tugraz.at
almbauer@ivt.tugraz.at
michael.lang@ivt.tugraz.at
zainer@ivt.tugraz.at

* Corresponding Author

ABSTRACT

Reed valves are widely used in hermetic reciprocating compressors for domestic refrigeration. They are crucial components in terms of efficiency, cooling performance, noise and reliability of the compressor. While reed valves already cause a significant proportion of the thermodynamic losses in fixed speed compressors, they induce even more challenges in variable speed compressors. Especially in variable speed compressors, a further improvement of the reed valve dynamics requires the consideration of a new valve concept.
In this work, a new design concept of a mechanically assisted suction valve is experimentally investigated. A mechanically actuated spiral spring generates a variable supporting force on the surface of a conventional reed valve. Experiments are conducted over a wide compressor speed range to determine how the new valve design contributes to the thermodynamic requirements of a variable speed compressor, which are high efficiency from low to medium compressor speed and high cooling capacity at high compressor speed. In addition, acoustic measurements will show the influence of the new design concept on noise, vibration and suction gas pulsation of the compressor.

1 INTRODUCTION

The refrigeration sector (including air conditioning) is estimated to require approximately 20 % of the global electrical energy consumption (IIR, 2019). Up to now, most of this electrical energy is produced by burning fossil fuels, which is associated with the emission of the greenhouse gas carbon dioxide. Making refrigeration systems more energy efficient would thus have a considerable influence on the reduction of the anthropogenic greenhouse effect and thereby help to meet the Paris Agreement from 2016.

In domestic refrigeration, mainly fixed speed hermetic reciprocating compressors are used to drive the refrigeration cycle. Variable speed operation is one effective approach to increase the energy efficiency of the entire refrigeration system. However, variable speed operation is associated with challenges concerning the reed valve dynamics. Reed valves are characterized by a simple and inexpensive design and by their automatic adaption to different operating conditions, as they are pressure actuated only. Reed valves are crucial compressor components in terms of efficiency, cooling capacity, noise and reliability. The main sources of thermodynamic losses are opening delays due to oil sticking and inertia effects, intermediate valve closings (valve flutter) and gas backflow due to valve closing delays.

Great efforts have been made in the past to analyze the relationship between reed valve dynamics and the compressor efficiency. The suction reed valve in particular shows a high flutter intensity, since the suction phase requires almost half a revolution of the crank shaft. Bhakta et al. (2012) conducted a sensitivity analysis of different suction valve parameters using a 1d compressor model. They emphasized the importance of reduced valve flutter for the reduction of valve losses. Similar findings were obtained by (Burgstaller et al., 2008). They investigated the potential of a theoretical valve without any flutter. The suction power consumption decreased by 36 % leading to a COP increase of 2 %. In variable speed operation, the suction time and discharge time varies with the compressor speed while the valve flutter frequency remains almost constant (Tan et al., 2014; Wang et al., 2016; Wang et al., 2012). This may lead to gas backflow due to delayed valve closure and thereby reduce the volumetric efficiency of the compressor (Nagata et al., 2010; Tao et al., 2018). Unlike the discharge valve, the suction valve lift is not limited by a stopper. Thus, increasing compressor speed leads to increased valve lifts and higher valve impact velocities, potentially provoking serious reliability issues.

Further improvements of the valve dynamics require the consideration of new valve concepts. An ideal suction reed valve opens fast, remains open during the entire suction phase and finally closes timely with a low valve impact velocity. Nevertheless, the automatic adaption to different operating conditions must be maintained. A first experimental attempt in this direction was made by Hopfgartner et al. (2017). The authors attempted to reduce the suction losses of a hermetic reciprocating compressor by using a negative preloaded suction reed valve in combination with an electromagnetic coil to support valve closure. Calorimeter measurements showed a COP improvement potential of up to 1.7 %. However, the COP improvement was strongly influenced by the operating condition and the energy consumption of the electromagnetic coil was not considered in the calculation. A different valve concept was proposed by (Egger et al., 2019). They investigated a mechanically assisted suction reed valve (MASV). Preliminary experimental investigations indicated a favorable behavior of the valve dynamics and calorimeter measurements at different operating conditions showed an average COP improvement of 1.9 %. Although the study has proven the functionality of the new valve concept, the proposed design is too costly and therefore not suitable for serial application. Therefore, Egger et al. (2020) proposed a new and cost-effective design of a MASV. The authors optimized the design using a simulation based multi-response optimization approach. In addition, some predicted improvements have already been confirmed in preliminary measurements of COP, cooling capacity and valve dynamics.

The present study provides an experimental investigation of the new and cost-effective MASV design. Not only calorimeter measurements, but also noise, vibration and suction gas pulsation measurements under various operating conditions provide a comprehensive insight into how the proposed MASV design affects the performance of a hermetic reciprocating compressor.

2 MECHANICALLY ASSISTED SUCTION REED VALVE

Figure 1 shows the components of the MASV. Although the design of the mechanism has been optimized for a small hermetic reciprocating compressor for domestic refrigeration, the principle can be applied to any other reciprocating compressor. The principle is based on an additional supporting force which acts on the conventional suction reed

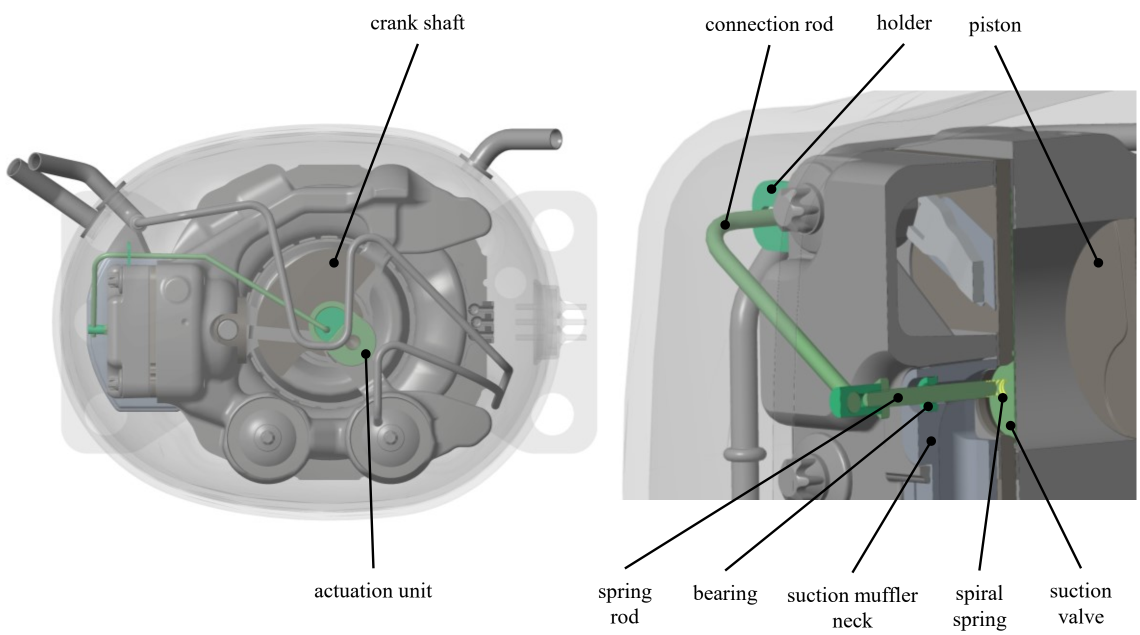

Figure 1: Components of mechanically assisted suction reed valve

valve, while the automatic adaption of the valve to different operating conditions is maintained. The magnitude of the supporting force must vary to ensure that the valve opens quickly, remains open during the entire suction phase and finally closes timely and with a low impact velocity. The valve support mechanism basically consists of a mechanical actuation unit, a connection rod and a spiral spring. The actuation unit drives the connection rod through an eccentric bore and thus leads to a sinusoidal motion of the spiral spring in valve opening direction. The compression of the spiral spring generates a variable force on the surface of the suction valve. The illustrated mechanism was designed in a way that enables fast changes of individual design parameters for experimental purposes. For example, the insert of the actuation unit can be changed in order to modify the amplitude and phase angle shift of the actuation. Furthermore, the distance offset between spiral spring and suction valve can be adjusted. No offset leads to a valve support duration of 180 °ca, while positive or negative offsets decrease or increase the support duration. Once all parameters are set, the mechanism design can be further simplified, e.g. the connection rod and the spring rod can be combined in one component.

3 EXPERIMENTAL APPROACH

The goal of this experimental investigation is to determine the influence of a new MASV design on the performance values i.e. COP, cooling capacity and acoustics over a wide compressor speed range and different operating conditions. The MASV design was selected on the basis of the investigations in (Egger et al., 2020), where several design variants are proposed. The underlying investigation is based on a MASV design which is composed of a valve support mechanism and the standard suction reed valve. Although this design variant does not lead to the best results over the entire compressor speed range, results similar to the optimal design variant are expected from low to medium compressor speeds (Egger et al., 2020) while, at the same time, requiring fewer modifications to the experimental unit.

3.1 Experimental Unit

The suction valve support mechanism was assembled on a commercially available hermetic reciprocating compressor for R600a with 9.6 cm^3 displacement and a cooling capacity of 171 W (ASHRAE test conditions, 220 V, 50 Hz). Figure 2 shows the experimental unit (without the upper shell cover) which was used for the experimental investigations. The most important design parameters of the tested valve support mechanism are shown in Table 1. The suction reed valve design remained the same in each measurement.

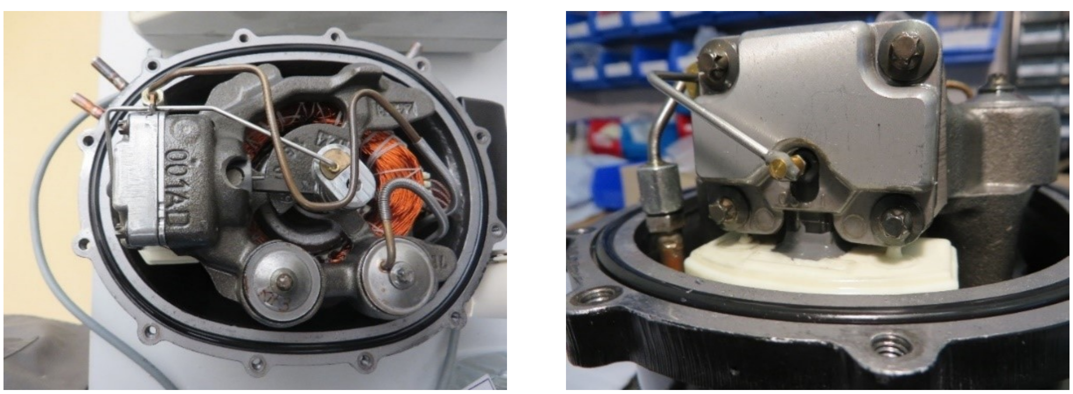

Figure 2: Hermetic reciprocating compressor equipped with a MASV (without upper shell cover)

Table 1: Design parameter of valve support mechanism

rod diameter (mm)	actuation amplitude (mm)	actuation phase angle shift 1) (°ca)	spiral spring offset 2) (mm)	spiral spring stiffness (N/mm)
2.0	1.5	0	0	2.0

1) crank angle offset to tdc at first contact between spiral spring and suction valve (having zero spiral spring offset)
2) distance offset between spiral spring and suction valve at tdc (having zero actuation phase angle shift)

3.2 Calorimeter measurements

A R600a secondary fluid calorimeter which complies with (ASHRAE, 2005) was used to determine the performance data i.e. cooling capacity, electrical power consumption and coefficient of performance (COP) of the compressor. The calorimeter automatically ensures stabilized operating conditions via an internal control unit. However, small deviations from the set point – still within the limits specified in (ASHRAE, 2005) – cannot be avoided. To account for this source of uncertainty, the measurement results were time averaged over 30 minutes measuring time. Furthermore, each operating condition was replicated three times. In addition to the standard compressor, two different variants based on the valve support mechanism in Table 1 were tested, see Table 2. Table 3 shows the different test conditions. Two different operating conditions in terms of evaporating and condensing temperature were tested at nominal compressor speeds starting from 2000 rpm up to 4500 rpm. The ambient temperature was kept constant at 32 °C. Based on the measurement results of the cooling capacity and electrical power consumption of the compressor, the COP is calculated according to equation 1. The results obtained with the MASV are given as relative change compared to the standard compressor, e.g. the COP change ΔCOP is calculated according to equation 2.

Table 2: Tested variants colorimeter measurements

variant name	MASV	suction bore diameter
standard	no	standard
var. C1	yes (see Table 1)	standard
var. C2	yes (see Table 1)	+ 7.5 %

Table 3: Test conditions calorimeter measurements

condition name (-)	evaporating temperature (°C)	condensing temperature (°C)	compressor speed (rpm)
-23.3°C/45°C	-23.3	45	2000 – 4500 (500rpm steps)
-23.3°C/55°C	-23.3	55	2000 – 4500 (500rpm steps)

$$COP = \frac{\dot{Q}_0}{\mathrm{P}_{el,comp}} \qquad (1)$$

$$\Delta COP_{variant} = 100 * \frac{COP_{variant} - COP_{standard}}{COP_{standard}} \qquad (2)$$

3.3 Acoustic measurements

Since the compressor is designed for domestic refrigerators and freezers, the acoustic behavior is another important quality criterion. In order to quantify the influence of the MASV on the acoustic behavior of the compressor, a total of three different variants as listed in Table 4 were tested with the compressor being operated in a reverberation room. In addition to the measurements of standard valve and MASV, a combination of both (var. A2) was tested to determine the acoustic influence of the small gap between the spring rod and the bearing in the suction muffler neck. Therefore, the spring rod was fixed in a position where no contact between the spiral spring and the suction valve could occur. A total of three different acoustic quantities were measured i.e. sound power level, shell vibration and suction gas pulsation. The sound power was determined according to DIN EN ISO 3741. Sound power and suction gas pulsation were measured simultaneously, while the shell vibration had to be measured separately, since the vibration sensors would influence the sound power level. All three measurements were conducted from 2000 rpm to 4500 rpm at two typical operating conditions for acoustic measurements, see Table 5.

Table 4: Tested variants acoustic measurements

variant name	MASV	suction bore diameter
standard	no	standard
var. A1	yes (see Table 1)	standard
var. A2	disabled [1)]	standard

[1)] to determine the acoustic influence of the small gap between the spring rod and the bearing in the suction muffler neck, the spring rod was fixed in a position where no contact between the spiral spring and the suction valve could occur.

Table 5: Test conditions acoustic measurements

condition name (-)	evaporating temperature (°C)	condensing temperature (°C)	compressor speed (rpm)
-25°C/55°C (LBP)	-25	55	2000 – 4500 (500rpm steps)
-10°C/40°C (MBP)	-10	40	2000 – 4500 (500rpm steps)

4 RESULTS

4.1 Calorimeter measurements

This chapter outlines the calorimeter measurement results i.e. COP, cooling capacity and electrical power consumption between 2000 rpm and 4500 rpm at two different operating conditions. The results are given for var. C1 and var. C2 as relative change compared to the standard compressor according to equation 2.

Figure 3 and Figure 4 show the relative COP change related to the compressor speed. Except for 4500 rpm at the second operating conditions, significant COP improvements are visible at both operating conditions over the entire compressor speed range. The first operating condition which corresponds to a condensing temperature of 45 °C shows slightly higher COP improvements than the second operating condition with 55 °C condensing temperature. This could be attributed to the fact that the optimization was carried out for the first operating condition in (Egger et al., 2020). Var. A2 shows higher COP improvements than var. A1 which is attributed to the enlarged suction bore. Furthermore, the difference between var. A1 and var. A2 increase with increasing compressor speed, which is plausible because the flow losses through the suction bore become more dominant at higher flow speeds. The largest COP improvement is about 3.6 % and can be observed at the first operating condition at 4000 rpm.

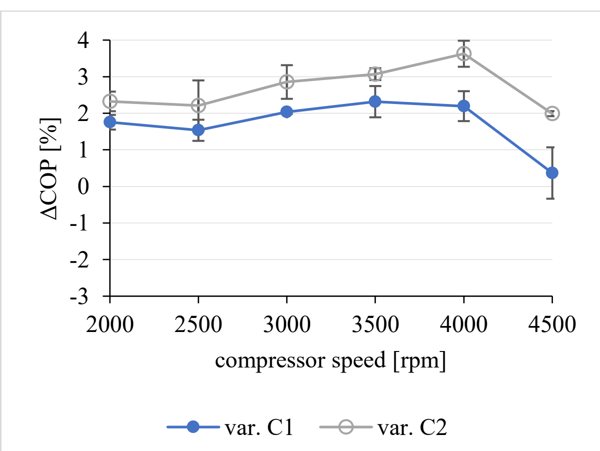

Figure 3: Change of COP over compressor speed at first operating condition (T_{evap} = - 23.3 °C, T_{cond} = 45 °C, T_{amb} = 32 °C, R600a)

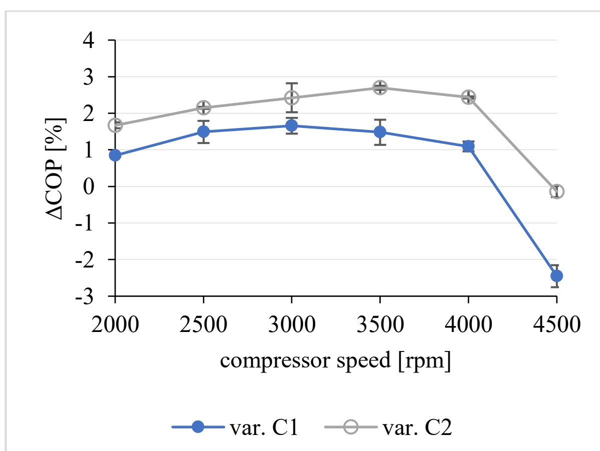

Figure 4: Change of COP over compressor speed at second operating condition (T_{evap} = - 23.3 °C, T_{cond} = 55 °C, T_{amb} = 32 °C, R600a)

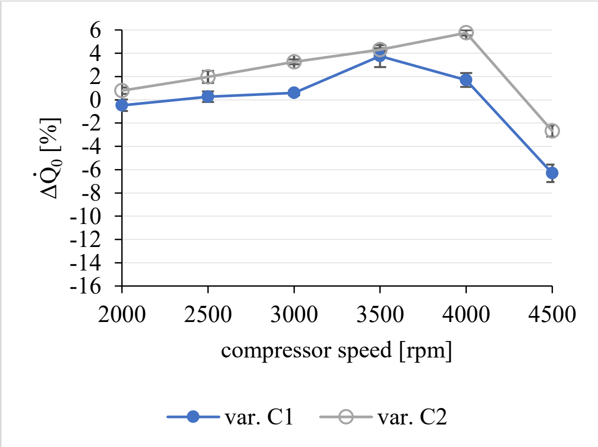

Figure 5: Change of cooling capacity at over compressor speed at first operating condition (T_{evap} = - 23.3 °C, T_{cond} = 45 °C, T_{amb} = 32 °C, R600a)

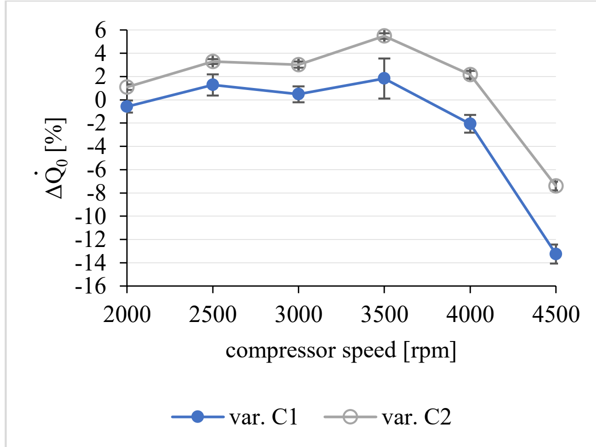

Figure 6: Change of cooling capacity over compressor speed at second operating condition (T_{evap} = - 23.3 °C, T_{cond} = 55 °C, T_{amb} = 32 °C, R600a)

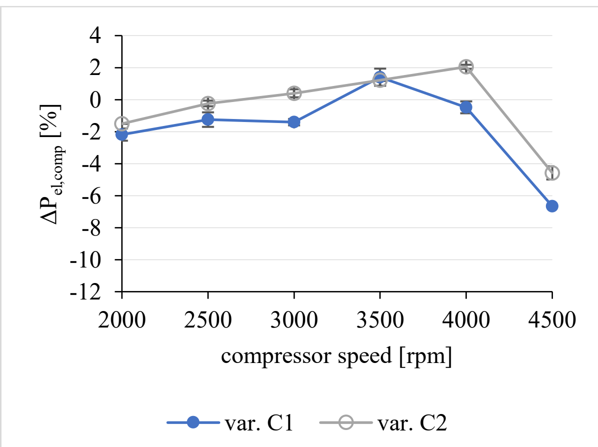

Figure 7: Change of electrical power consumption over compressor speed at first operating condition (T_{evap} = - 23.3 °C, T_{cond} = 45 °C, T_{amb} = 32 °C, R600a)

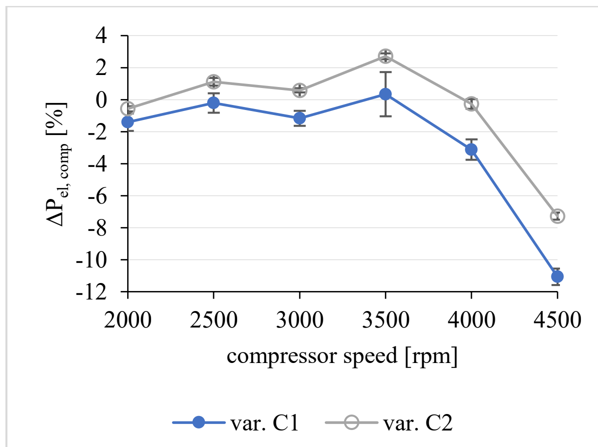

Figure 8: Change of electrical power consumption over compressor speed at second operating condition (T_{evap} = - 23.3 °C, T_{cond} = 55 °C, T_{amb} = 32 °C, R600a)

Figure 5 and Figure 6 illustrate the relative change of the cooling capacity related to the compressor speed. In general, the cooling capacity curves of both variants show a similar trend as the corresponding COP curves in Figure 3 and Figure 4. This is not surprising as the cooling capacity is directly included in the calculation of the COP according to equation 1. At the first operating condition, var. C2 shows a continuous increase in cooling capacity improvement from 2000 rpm up to 4000 rpm, with a maximum improvement of 5.8 % at 4000 rpm. At maximum compressor speed however, var. C1 and var. C2 show lower cooling capacities than the standard compressor. This is in accordance with the findings in (Egger et al., 2020), where the simulation indicated weak valve dynamics at high compressor speeds if the valve support mechanism is combined with the standard suction reed valve.

Figure 7 and Figure 8 show the relative change of the electrical power consumption of the compressor related to the compressor speed. The electrical power consumption depends strongly on the mass flow and thus also on the cooling capacity of the compressor. An increase in cooling capacity is associated with an increase in electrical power consumption. The effect of the MASV is clearly visible when comparing the electrical power consumption in Figure 7 and Figure 8 with the cooling capacity in Figure 5 and Figure 6. Some results with cooling capacity changes close to zero nevertheless show significant reductions in electrical power consumption, e.g. var. C1 at first operating condition and 2500 rpm.

4.2 Acoustic measurements

a) Sound power level

Figure 9 and Figure 10 show the compressor sound power level in the frequency domain (one-third octave spectrum) at LBP and MBP at low (2000 rpm) and high (4500 rpm) compressor speed. In general, higher compressor speeds lead to higher sound power levels and smaller differences between the individual variants. At 2000 rpm, var. A1 shows significant higher sound power levels between 2500 Hz and 6300 Hz than var. A2 and the standard compressor. Since var. A2 has similar levels as the standard compressor, it is likely that the increased noise of var. A1 is caused by the mechanism movement and not by the small gap in the suction muffler neck. Figure 11 and Figure 12 show the total sound power level related to the compressor speed at LBP and MBP. It turns out, that at LBP, from low to medium compressor speeds, var. A1 leads to considerable higher total sound power levels than the standard compressor, which is in accordance with Figure 9. At MBP, however, the differences between the individual variants are small. Furthermore, at a given compressor speed, var. A1 shows smaller differences in sound power level between LBP and MBP than the standard compressor. In general, it can be said that the influence of the compressor speed on the sound power level is much greater than the influence of the MASV.

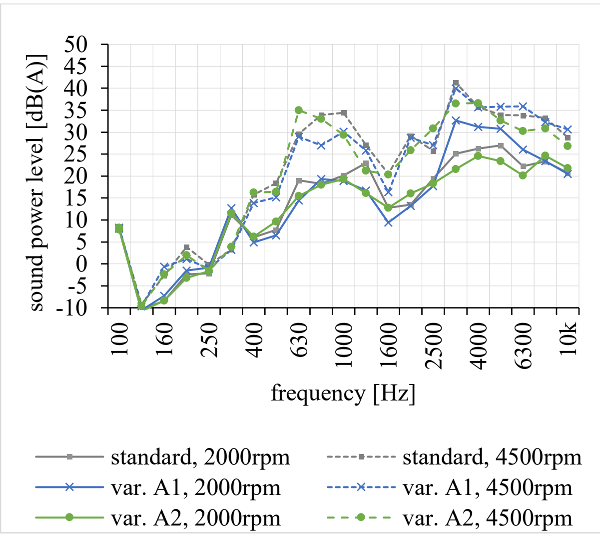

Figure 9: Compressor sound power level at LBP, 2000 rpm and 4500 rpm

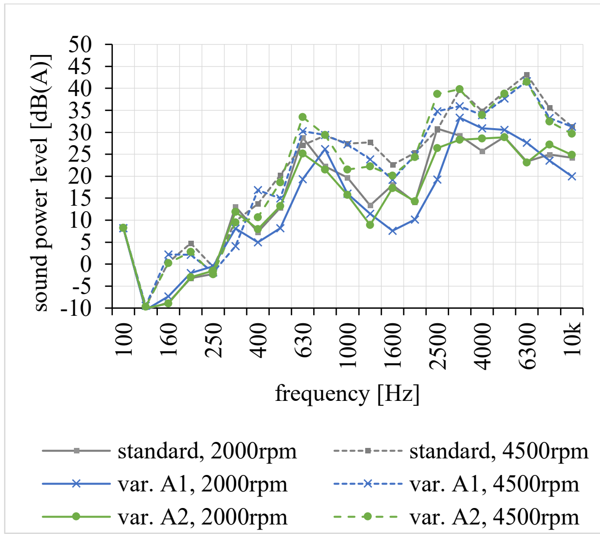

Figure 10: Compressor sound power level at MBP, 2000 rpm and 4500 rpm

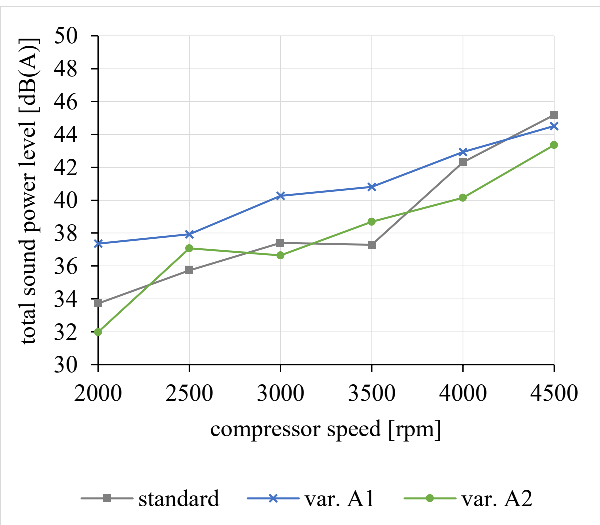

Figure 11: Total sound power level of compressor from 2000 rpm to 4500 rpm at LBP

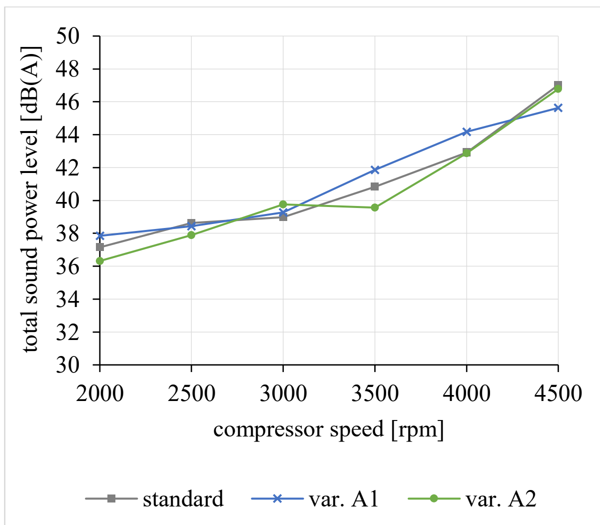

Figure 12: Total sound power level of compressor from 2000 rpm to 4500 rpm at MBP

b) Vibration

Figure 13 and Figure 14 show the compressor shell vibration in the frequency domain at LBP and MBP at low and high compressor speed. Both plots have a logarithmic ordinate due to the large differences in the size of the vibration values. The highest peaks occur near the operating frequency of the compressor, i.e. 33.3 Hz and 75 Hz for 2000 rpm and 4500 rpm respectively. No difference between the tested variants can be observed at these operation frequency related vibration peaks. The remaining frequency range of var. A1 is characterized by slightly higher and slightly lower vibration values compared to the standard compressor. The largest difference occurs at MBP and 2000 rpm near 630 Hz, where var. A1 has a significantly lower vibration value. However, considering the whole frequency spectrum, no general improvement or worsening of the MASV (var. A1) can be observed. The small gap in the suction muffler neck caused by the bearing of the spring rod seems to have a neglectable effect on the vibration, because var. A2 has similar vibration values as the standard compressor.

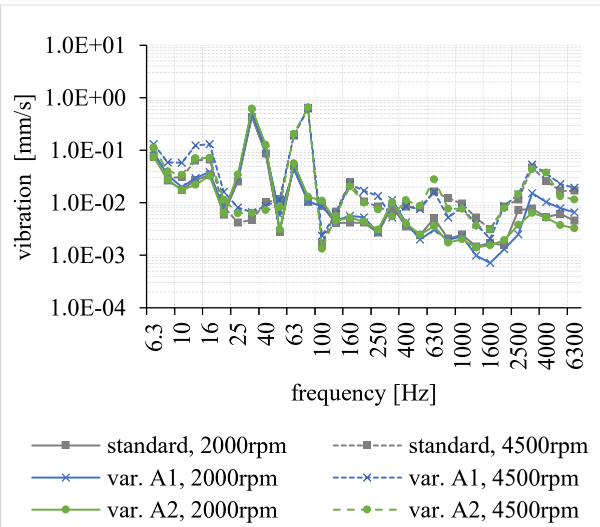

Figure 13: Shell vibration at LBP, 2000 rpm and 4500 rpm

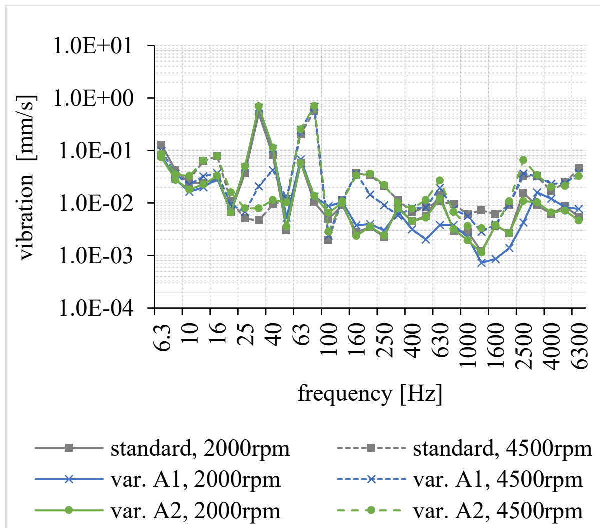

Figure 14: Shell vibration at MBP, 2000 rpm and 4500 rpm

c) Suction gas pulsation

Figure 15 and Figure 16 show the suction gas pulsation in the frequency domain at LBP and MBP at low and high compressor speed.

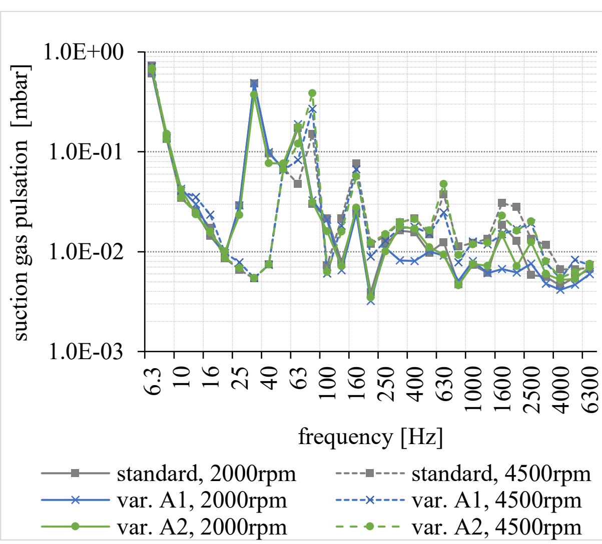

Figure 15: Suction gas pulsation at LBP, 2000 rpm and 4500 rpm

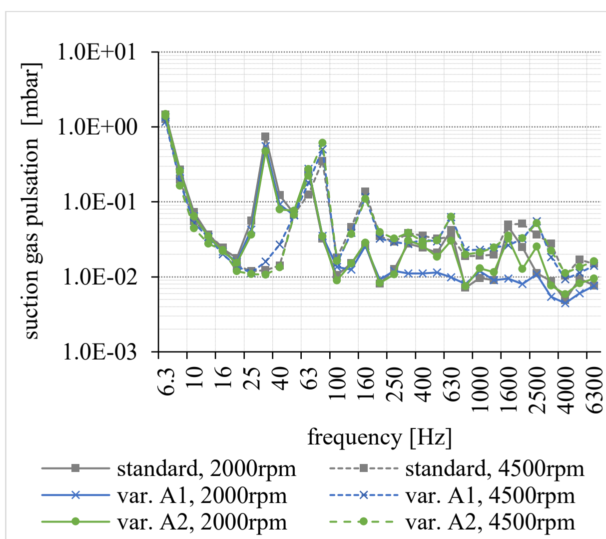

Figure 16: Suction gas pulsation at MBP, 2000 rpm and 4500 rpm

As with the shell vibration measurement, the largest peaks in suction gas pulsation occur at the operating frequency of the compressor. At 2000 rpm a significant reduction of the suction gas pulsation between 250 Hz and 4000 Hz can be observed at both operating conditions. At 4500 rpm the reduction is slightly less pronounced. This could be due to the fact that higher compressor speeds lead to fewer intermediate valve closings, as the suction time decreases while the valve flutter frequency remains the same. Also, with regard to suction gas pulsation, the small gap in the suction muffler neck seems to be neglectable.

5 CONCLUTION AND OUTLOOK

The influence of a new and cost-effective MASV design on the performance values of a hermetic reciprocating compressor has been experimentally investigated. Not only calorimeter measurements, but also acoustic measurements were conducted from 2000 rpm up to 4500 rpm at various operating conditions to determine the effect on COP, cooling capacity and electrical power consumption, noise, vibration and suction gas pulsation of the compressor.

Calorimeter measurements indicate a significant increase of the COP at almost every compressor speed and operating condition when using the MASV. The highest COP improvements, up to 3.6 %, are obtained if the MASV is combined with an enlargement of the suction bore. In the standard compressor, a suction bore enlargement is hardly feasible, as it usually increases the valve impact velocity, which is already close to the limit from reliability perspective. However, as proved in (Egger et al., 2020; Egger et al., 2019) a MASV significantly reduces the valve impact velocity, making a suction bore enlargement feasible. Not only the COP, but also the cooling capacity can be increased with the MASV. As with the COP, the highest cooling capacity improvements are obtained if the MASV is combined with a suction bore enlargement. From low to medium compressor speeds, the cooling capacity improvements tend to increase with increasing compressor speed. At 4500 rpm, however, a strong decline in cooling capacity can be observed at both tested operating conditions. In principle, the MASV concept would be able to improve COP and cooling capacity even at high compressor speeds, but this would require a suction reed valve with different valve parameters (Egger et al., 2020).

The acoustic measurements indicate that, when using a MASV, the sound power level of the compressor increases considerably at LBP from low to medium compressor speeds. This can be attributed to the motion of the valve support mechanism and most likely has its origin in the bearing points. At MBP, which is usually the noisier operating condition, the total sound power level of the compressor equipped with the MASV remains almost the same as at LBP. This is why at MBP no significant differences in total sound power level between standard and MASV can be observed. The shell vibration measurement indicated no fundamental changes when using the MASV, while the suction gas pulsation between 250 Hz and 4000 Hz at 2000 rpm was significantly reduced.

Future work will be focused on a further investigation of the noise coming from the valve support mechanism as well as a measurement-based Design of Experiment approach to determine the effect of different design factors on COP and cooling capacity of the compressor.

NOMENCLATURE

COP	coefficient of performance
ΔCOP	relative change of coefficient of performance
$P_{el,comp}$	electrical power consumption of compressor
$\Delta P_{el,comp}$	relative change of electrical power consumption of compressor
$\dot{Q}_0$	cooling capacity
$\Delta\dot{Q}_0$	relative change of cooling capacity

Abbreviations

amb	ambient
ca	crank angle
cond	condensing
evap	evaporating

LBP low back pressure
MASV mechanically assisted suction reed valve
MBP medium back pressure
rpm revolutions per minute
var variant
1d one-dimensional

ACKNOWLEDGEMENTS

This research was supported by the Austrian Research Promotion Agency (FFG) under the reference number 861517 and by Secop GmbH.

6 References

American Society of Heating, Refrigerating and Air-Conditioning Engineers, 2005. ANSI/ASHRAE Standard 23-2005: Methods of Testing for Rating Positive Displacement Refrigerant Compressors and Condensing Units. Atlanta, Ga.

Bhakta, A., Dhar, S., Bahadur, V., Angadi, S., Dey, S., 2012. A Valve Design Methodology For Improved Reciprocating Compressor Performance. International Compressor Engineering Conference.

Burgstaller, A., Nagy, D., Almbauer, R., Lang, W., 2008. Influence of the Main Parameters of the Suction Valve on the Overall Performance of a Small Hermetic Reciprocating Compressor. International Compressor Engineering Conference.

Egger, A., Almbauer, R., Dür, L., Hopfgartner, J., Lang, M., 2020. Multi-Response optimization applied to a mechanically assisted reed valve of a hermetic reciprocating compressor. International Journal of Refrigeration 119, 119–130. https://doi.org/10.1016/j.ijrefrig.2020.07.008.

Egger, A., Almbauer, R., Dür, L., Hopfgartner, J., Zuber, B., Stangl, S., 2019. Experimental Investigation of a Mechanically Assisted Suction Reed Valve in a Small Hermetic Reciprocating Compressor. IOP Conference Series: Materials Science and Engineering 604, 12018. https://doi.org/10.1088/1757-899x/604/1/012018.

Hopfgartner, J., Posch, S., Zuber, B., Almbauer, R., Krischan, K., Stangl, S., 2017. Reduction of the suction losses through reed valves in hermetic reciprocating compressors using a magnet coil. IOP Conference Series: Materials Science and Engineering 232, 12034. https://doi.org/10.1088/1757-899x/232/1/012034.

IIR, 2019. The Role of Refrigeration in the Global Economy. 38th Note on Refrigeration Technologies. https://iifiir.org/en/fridoc/142028.

Nagata, S., Nozaki, T., Akizawa, T., 2010. Analysis of Dynamic Behavior of Suction Valve Using Strain Gauge in Reciprocating Compressor. International Compressor Engineering Conference.

Tan, Q., Pan, S.-l., Feng, Q.-k., Yu, X.-l., Wang, Z.-l., 2014. Fluid–structure interaction model of dynamic behavior of the discharge valve in a rotary compressor. Proceedings of the Institution of Mechanical Engineers, Part E: Journal of Process Mechanical Engineering 229 (4), 280–289. https://doi.org/10.1177/0954408914530122.

Tao, W., Guo, Y., He, Z., Peng, X., 2018. Investigation on the delayed closure of the suction valve in the refrigerator compressor by FSI modeling. International Journal of Refrigeration 91, 111–121. https://doi.org/10.1016/j.ijrefrig.2018.05.004.

Wang, F., Mu, G., Guo, Q., 2016. Design optimization of compressor reed valve based on axiomatic design. International Journal of Refrigeration 72, 132–139. https://doi.org/10.1016/j.ijrefrig.2016.07.019.

Wang, Y., Feng, J., Zhang, B., Peng, X., 2012. Modeling the valve dynamics in a reciprocating compressor based on two-dimensional computational fluid dynamic numerical simulation. Proceedings of the Institution of Mechanical Engineers, Part E: Journal of Process Mechanical Engineering 227 (4), 295–308. https://doi.org/10.1177/0954408912465366.